ADVANCED SUSTAINABLE SYSTEMS
www.advsustainsys.com

Sustainable Liquid Luminescent Solar Concentrators

Ana R. Frias, Sandra F. H. Correia, Margarida Martins, Sónia P. M. Ventura, Edison Pecoraro, Sidney J. L. Ribeiro, Paulo S. André, Rute A. S. Ferreira, João A. P. Coutinho, and Luís D. Carlos**

Luminescent solar concentrators (LSCs) are photovoltaic (PV) complementary devices to overcome the mismatch between the Si-based PV cells, response and the solar spectrum, allowing PV urban integration. Challenges for the luminescent layer include the use of abundant and sustainable natural organic molecules. Here, LSCs composed of a glass container and based on bundles of cylindrical hollow-core plastic optical fibers filled with aqueous solutions of R-phycoerythrin (R-PE), extracted from Gracilaria sp. algae are presented. The R-PE solutions absorb in the UV/visible spectral range (300–550 nm) and convert this radiation into red-emission (550–700 nm) with a maximum absolute quantum yield of ≈0.39. In this work, LSCs with distinct geometries are reported, in which the R-PE emission yields optical conversion efficiency values up to ≈6.88% and ≈4.74% for a planar device and for a bundle of cylindrical LSCs, respectively, which are the largest values known for liquid-based LCSs using sustainable emitting centres. Moreover, the coupling of the LSCs to commercial Si-based PV devices yields power conversion efficiency values of ≈0.27% (planar) and ≈23.03 × 10^{-3}%, (bundle). These values illustrate the potential of this approach for the development of natural-based LSCs meeting the requirements of reliable, sustainable, and competitive energy systems.

1. Introduction

Luminescent solar concentrators (LSCs) appeared in the late 1970s with the goal of overcoming the mismatch between the full solar spectrum on Earth and the absorbance one of the semiconductor material used in the photovoltaic (PV) cell manufacture.[1] The first reported examples are planar devices[2–5] (p-LSCs) containing optical active centres able to complement the absorption of the PV cell and emission in the PV cell absorption spectral range. Given the refractive index contrast between the LSC surface and the air, the emitted radiation is guided in the LSC by total internal reflection to PV cells located at its edges.[2,6] Other relevant aspect of the LSC operation is that analogous performance is expected under direct or diffuse light incidence,[7–9] permitting to prospect the use of PV panels under cloudy conditions, which is a significant advantage for integration of PV cells in urban buildings. As an illustrative example of the real-world applicability of these devices, we highlight the implementation of large scale LSC-based panels in a noise barrier configuration as outdoors alongside a roadway in the Netherlands.[10–12] Other applications are envisaged in PV urban integration, as LSCs are attractive to contribute to zero-energy buildings in which the LSCs are embedded in façades, or windows.[13–15]

Furthermore, LSCs are candidates to contribute in mobile energy, as they may be integrated in wearable fabrics and outdoor furniture.[16] In particular, target delivered power values up to 10 W may be feasible with the actual figures of merit for LSCs, allowing to charge low-voltage devices, e.g., mobile

A. R. Frias
Department of Physics
CICECO—Aveiro Institute of Materials and Instituto de Telecomunicações
University of Aveiro
3810-193 Aveiro, Portugal
Dr. S. F. H. Correia, Prof. R. A. S. Ferreira, Prof. L. D. Carlos
Department of Physics and CICECO—Aveiro Institute of Materials
University of Aveiro
3810-193 Aveiro, Portugal
E-mail: rferreira@ua.pt; lcarlos@ua.pt
M. Martins, Dr. S. P. M. Ventura, Prof. J. A. P. Coutinho
Department of Chemistry and CICECO—Aveiro Institute of Materials
University of Aveiro
3810-193 Aveiro, Portugal
The ORCID identification number(s) for the author(s) of this article can be found under https://doi.org/10.1002/adsu.201800134.
Dr. E. Pecoraro, Prof. S. J. L. Ribeiro
UNESP—Institute of Chemistry
São Paulo State University
P.O. Box 355, 14801-970 Araraquara-SP, Brazil
Prof. P. S. André
Department of Electric and Computer Engineering
Instituto Superior Técnico
Universidade de Lisboa
1049-001 Lisboa, Portugal
Prof. P. S. André
Instituto de Telecomunicações
University of Aveiro
3810-193 Aveiro, Portugal

DOI: 10.1002/adsu.201800134

phones, sensors, and wi-fi routers.[17] In what concerns mobile energy, cylindrical-based LSCs (c-LSCs) assembled in bundles[18] may offer additional advantages arising from the intrinsic properties of the fibers themselves, such as being lightweight, flexible, and may be coupled to other optical fibers for light waveguiding, which may allow remote light harvesting. Theoretical studies point out a decrease of the optical losses (through reflection) in the case of a bundle structure, when compared to a planar LSC.[19] Additionally, from an experimental point of view, LSCs based on bundles displayed enhanced performance, when compared with that of planar LSC with analogous surface collection area and light harvesting absorbance, due to the individual waveguiding features of each fiber that contributes to reduce the reabsorption losses.[20]

Regarding the material selection toward LSC performance optimization, several challenges are still open. Different optically active centres have been tested in LSCs, as reviewed in some works,[21–23] including organic dyes, quantum dots (QDs), Ln^{3+} ions, and, more recently, metal halide clusters.[24] The best performance single-layer LSC is based on perylimide with optical conversion efficiency values (η_{opt}, defined as the ratio between the output optical power, P_{out}, and the incident optical power, P_{in}) of 18.8%.[25] Despite the small Stokes-shift of organic dyes, they present high emission quantum yields and large absorption coefficients,[26] which result in better performance LSC devices, when compared with LSCs based on other optically active centres.

The potential replacement of synthetic organic dyes by luminescent organic molecules extracted from renewable and natural materials could make LSCs cheaper and sustainable, keeping other inherent features such as synthetic versatility, high absorption coefficients, and emission quantum yields.[27,28] As a matter of fact, previous studies proved the advantages and the possibility of using natural and renewable materials for energy harvesting[29] and, specifically, for LSCs.[30] The most common natural dyes used in LSCs are based on phycobilisomes.[28,31,32] These are photosynthetic complexes, mainly composed of phycobiliproteins, with light-harvesting ability over a broad range of the visible spectrum and which concentrate the captured energy at the photosynthetic reaction center.[31,33,34] Nevertheless, studies reporting natural dye molecules for LSCs are scarce. A recent example reports the use of Boron-dipyrromethene emitter covalently linked to oligofluorene and dispersed in lauryl methacrylate and ethylene glycol dimethacrylate, which when coupled to Si PV cells yielded an external quantum efficiency (EQE) maximum value of ≈2.44%.[28] Another p-LSC example is based on phycobilisomes dispersed in acrylamide films,[31,34] which presented η_{opt} = 12.5%.[31] In this study, the use of phycobilisomes in liquid medium confined in a glass cuvette was also tested, but considered disadvantageous due to the refractive index mismatch between the solution and the cuvette.[34]

Several LSCs based on optically active centres dispersed in a liquid medium have been proposed in literature,[8,31,34–43] but studies reporting LSCs performance quantification (η_{opt}, EQE or power conversion efficiency, PCE) are not abundant.[40–42,44,45] The maximum η_{opt} values were found for PbS QDs dispersed in toluene (η_{opt} = 12.6%, considering collection along the four edges)[42] and for K_I organic dye dispersed in a liquid polymer (η_{opt} = 20.2% for direct radiation).[40] Very recently, an interesting work reporting temperature-responsive LSCs using a liquid crystal as host for a coumarine-derivative/perylene bisimide pair with η_{opt} = 2.4% in the cold state and η_{opt} = 3.2% when warmed was published, stating the potential for LSCs with liquid optically active layers.[44] Despite the advantages of biobased dyes in liquid medium, only one report mentions the use of phycobilisomes in liquid medium for LSCs however, without mentioning any performance quantification.[34]

Among the natural dyes, phycobilisomes are very promising, since donor and acceptor molecules are already aggregated in an ideal configuration,[34] and phycobiliproteins can be efficiently extracted, without compromising their conformational structure or chromophore structural integrity through a method already reported by some of us.[46] Moreover, R-phycoerythrin (R-PE), which is one of the most abundant phycobiliproteins in red macroalgae, has been pointed out as an important macromolecule in the field of medical diagnosis and biomedical research[47] due to its high absorption coefficient and emission quantum yield.[46] Recently, laser effect was observed from R-PE from 602 to 620 nm with pulsed optical excitation in a Fabry–Pérot resonator.[48]

In this work, we merge two complementary aspects toward enhanced performance sustainable LSCs devices: i) the use of R-PE, extracted from fresh *Gracilaria sp*. red algae and dispersed in an aqueous solution and ii) the exploiting of the geometrical factor fabricating c-LSCs based on bundles of cylindrical hollow-core polymethylmethacrylate (PMMA)-optical fibers (POFs) (**Figure 1**A) and p-LSCs composed of a glass container (Figure 1B). The scalability and economic feasibility of the proposed methodology is granted from both the selection of PMMA and the R-PE. In particular, the substrate is based on PMMA-based optical fibers processed using a semi-industrial facility able to pull meter-length fibers as already reported by some of us.[49] Moreover, the use of PMMA is a very interesting and practical approach to reduce the price of LSCs because it is one of the most used polymers and thus production methods are quite efficient and cost-effective.[50,51] The use of *Gracilaria sp*. algae takes advantage of local resources and markets. The fact of being dispersed in water makes this approach sustainable and without waste nor significant negative impact toward the environment. Moreover, the use of aqueous solutions to extract phycobiliproteins from the fresh biomass can also be easily integrated with further steps of downstream processing by using, for example, conventional liquid–liquid extraction or the alternative aqueous biphasic systems,[52] which can be easily scaled-up (also) to continuous flow. Different concentrations (0.4×10^{-7}–17×10^{-7} M) of R-PE in aqueous solutions with high molar brightness (B) values (2.2×10^{5}–6.2×10^{5} M^{-1} cm^{-1}) were used to fabricate c-LSCs (Figure 1A) and p-LSCs (Figure 1B). Electrical measurements were performed in coupled c-Si PV devices, yielding maximum η_{opt} values of ≈6.88% (p-LSC) and ≈4.74% (c-LSCs bundle), and PCE of ≈0.27% (p-LSC) and ≈23.03×10^{-3}% (c-LSCs bundle).

2. Results and Discussion

2.1. Optical Characterization of the R-PE Solutions

Figure 2 shows the emission spectra of the R-PE based aqueous solutions, which are formed by a broad band typical of R-PE

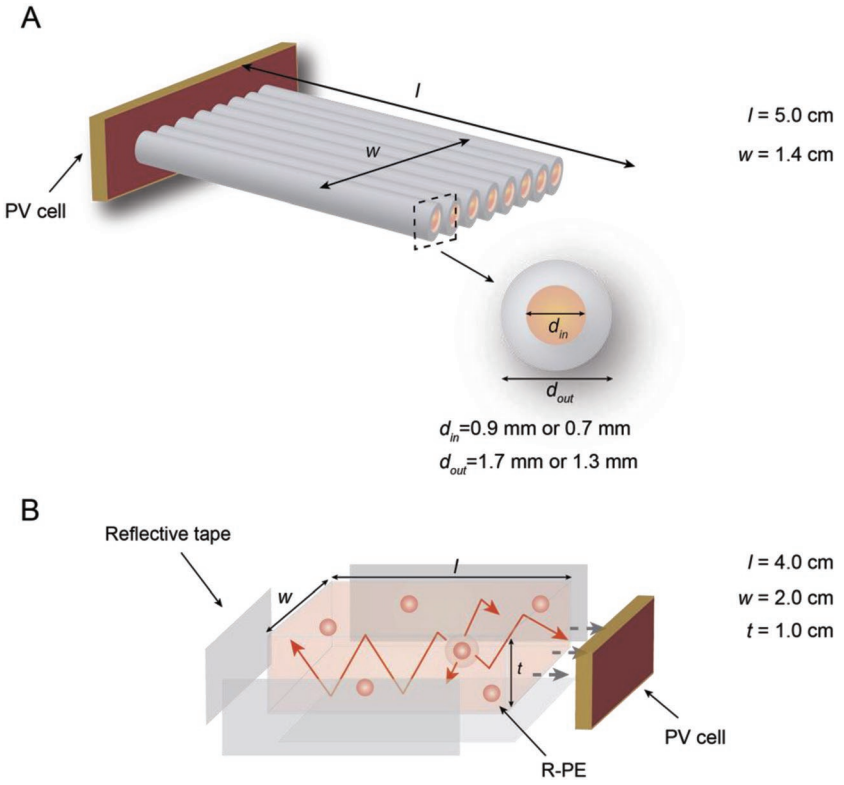

Figure 1. Scheme of the A) fiber c-LSCs bundle structure and B) p-LSC.

fluorescence,[46] whose relative intensity depends on the dye concentration. For the less concentrated solutions (0.4×10^{-7}–3.3×10^{-7} M), the room-temperature emission spectra are dominated by the R-PE characteristic emission with two components centred around 577 and 632 nm. The presence of two distinct dye-related components in the emission spectrum points out the formation of dye aggregates.[53] In fact, by increasing the concentration, the relative intensity of the low-energy component (655 nm) increases and the main peak (577 nm) red-shifts around 6 nm, suggesting the presence of *J*-dimers.[54]

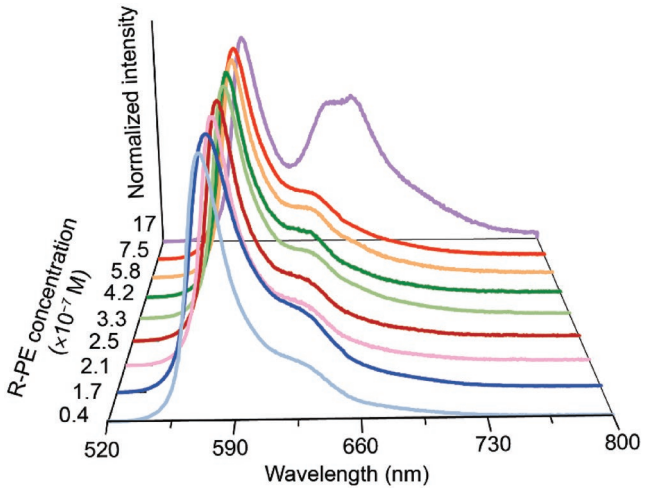

Figure 2. Emission spectra of the R-PE solutions excited at 498 nm.

The excitation spectra (Figure S1A in the Supporting Information) are dominated by the excited states of the R-PE in the visible spectral range, revealing also the presence of components in the UV/blue (320–440 nm) attributed to the chromophores' singlet states. The band at 278 nm arises from amino acid residues of the apoprotein.[55]

The emission properties of the samples were also quantified through the measurement of the absolute emission quantum yield (*q*, **Table 1**), as function of the excitation wavelength (310–540 nm). Although a maximum emission quantum yield is observed under excitation in the visible range (498 nm), as the concentration is increased, this value decreases from 0.37 ± 0.04 (0.4×10^{-7} M solution) to 0.16 ± 0.02 (17×10^{-7} M solution). These values are lower than those previously reported on literature of 0.82–0.85,[56,57] found for R-PE in phosphate buffers and for less concentrated samples (≈10^{-15} M).[56]

The light-harvesting ability of all the R-PE aqueous solutions relative to the AM1.5G spectrum (**Figure 3**A) was studied by absorption spectroscopy. Figure 3B shows the absorption spectra of three selected R-PE aqueous samples (absorption spectra of all samples in Figure S1B in the Supporting Information), which resemble the excitation spectra above mentioned, apart from the presence of a component around 590–690 nm, probably ascribed to the presence of other phycobiliproteins, such as phycocyanin and allophycocyanin.[31] There are no significant spectral changes in the absorption spectra as the concentration is varied, although the absolute absorbance value increases with concentration (Figure 3B; Figure S1B in the Supporting Information). The absorbance dependence on the concentration was rationalized by the calculation of the molar extinction coefficient values (*ε*, Table 1), revealing that with exception of the low-concentrated solution (0.4×10^{-7} M), analogous values within 1.3–1.9 × 10^6 M^{-1} cm^{-1} were found, in good agreement with previous studies in literature.[56,57] Moreover, in order to quantify the ability of the LSCs to absorb the sunlight available for PV conversion, the overlap integral between the R-PE solutions absorption spectra and the solar irradiation on Earth was calculated[58]

$$O = \int_{\lambda_1}^{\lambda_2} N_{\mathrm{AM1.5G}}(\lambda) \times \left(1 - 10^{-A(\lambda)}\right) \mathrm{d}\lambda \quad (1)$$

where λ_1 and λ_2 are the limits of the spectral overlap between the absorption spectrum of the R-PE solution and the AM1.5G spectrum, $N_{\mathrm{AM1.5G}}$ is the photon flux of AM1.5G and *A* is the absorbance of the R-PE solution. The *O* values increase with the concentration (Figure 3C and Table 1). The maximum calculated *O* value indicates that the 17×10^{-7} M aqueous solution has the potential to absorb ≈27% of the solar photon flux on the Earth (4.3×10^{21} photons s^{-1} m^{-2}).[58]

Table 1. Integral overlap (O, photons s^{-1} m^{-2}), molar extinction coefficient (ε, M^{-1} cm^{-1}), absolute emission quantum yield (q), and brightness (B, M^{-1} cm^{-1}) as function of the R-PE concentration ([ ], M). The ε, q, and B values refer to 498 nm.

[ ] ($\times 10^{-7}$)	O ($\times 10^{20}$)	ε ($\times 10^{6}$)	q	B ($\times 10^{5}$)
0.4	0.9	1.7	0.37 ± 0.04	6.2
1.7	2.1	1.0	0.39 ± 0.04	3.9
2.1	3.0	1.3	0.34 ± 0.03	4.2
2.5	3.8	1.4	0.32 ± 0.03	4.5
3.3	4.8	1.4	0.30 ± 0.03	4.0
4.2	5.5	1.4	0.28 ± 0.03	3.7
5.8	6.9	1.5	0.25 ± 0.03	3.8
7.5	8.0	1.6	0.24 ± 0.02	3.2
17	10.4	1.5	0.16 ± 0.02	2.2

Light emission efficiency and light harvesting ability can be related by the B parameter, given by $B = q \times \varepsilon$,[59] allowing both properties to be compared for distinct samples. The B values were calculated as function of the R-PE concentration (Table 1), and are one order of magnitude larger than those reported for other organic-dye molecules, with light emission in the 530–650 nm range.[60,61] We note that the larger B values are found in the R-PE concentration region between 2.1×10^{-7} and 5.8×10^{-7} M. At higher concentrations (7.5×10^{-7} and 17×10^{-7} M), B decreases due to the concentration quenching, as suggested by the emission spectra analysis. At lower concentrations (0.4×10^{-7} and 1.7×10^{-7} M), the q values are higher, resulting in larger B values although the absorption coefficient is decreased.

Taking advantage of the ability of the R-PE solutions to harvest the AM1.5G radiation and convert it into visible emission, the solutions were incorporated into hollow core POFs (**Figure 4**A), permitting the fabrication of c-LSCs based on natural dyes in a liquid medium. The fabrication of these short-length c-LSCs aims at establishing the potential to design large area flexible (**Figure 5**; Figure S2 in the Supporting Information) and transparent (Figure S3 in the Supporting Information) c-LSCs made from the assembling of POFs filled with the R-PE aqueous solution in bundle structures. We notice the transparency of the bundles arising from the high transmittance of the PMMA.[62] As **Figure 6**A illustrates, when illuminated by AM1.5G solar radiation, the orange-red emission of the R-PE based solutions is guided to the edges of the device through total internal reflection. Also, as evidenced in Figure 6B,C, the emission intensity guided in the PMMA cladding is larger (≈2 times) than that in the hollow-core (further details in the Supporting Information).

The relative performance of the c-LSCs based on a single POF was quantified by the calculation of the η_{opt} and PCE. The quantification of η_{opt} from the experimental data is attained in different ways in the literature. In this work, we used the definition given by[25]

$$\eta_{opt} = \frac{P_{out}}{P_{in}} = \frac{I_{SC}^{L} V_{0}^{L}}{I_{SC} V_{0}} \frac{A_e}{A_s} \frac{\eta_{solar}}{\eta_{PV}} \quad (2)$$

where I_{SC}^{L} and V_{0}^{L} represent the short-circuit current and the open-circuit voltage when the PV device is coupled to the LSC (I_{sc} and V_0 are the corresponding values of the PV device exposed directly to the solar radiation), η_{solar} is the efficiency of the PV device relatively to the total solar spectrum and η_{PV} is the efficiency of the PV device at the LSC emission wavelengths (experimental details can be found in the Supporting Information). The maximum η_{opt} values (0.16 ± 0.02%, for $G \approx 7$) were found for concentration solutions within 2.5×10^{-7} to 5.8×10^{-7} M (Table S1 in the Su`pporting Information). To enable a comparison with the literature, an alternative definition will be also considered[41]

$$\eta_{opt} = \frac{I_{SC}^{L}}{I_{SC}} \frac{A_e}{A_s} \quad (3)$$

The PCE was calculated as follows

$$PCE = \frac{P_{out}^{el}}{P_{in}} = \frac{I_{SC}^{L} V_{0}^{L} FF}{A_S \int_{\lambda_1}^{\lambda_2} I_{AM1.5G}(\lambda) d\lambda} \quad (4)$$

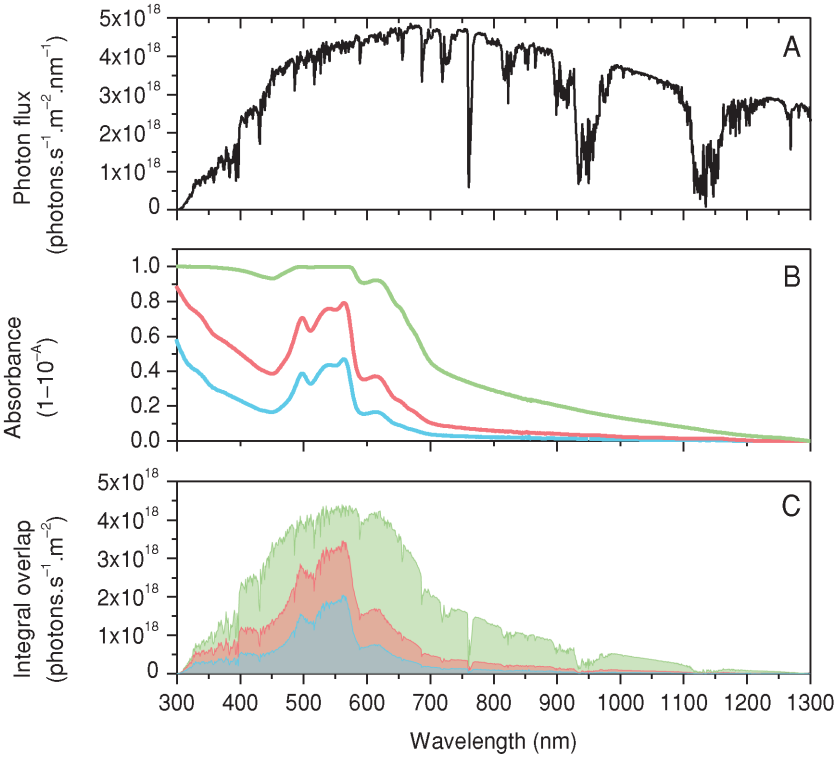

Figure 3. A) Solar photon flux on Earth at AM1.5G, B) absolute absorbance of 1.7×10^{-7} M (blue line), 3.3×10^{-7} M (red line), and 17×10^{-7} M (green line), and C) integral overlap between the solar photon flux and the absolute absorbance.

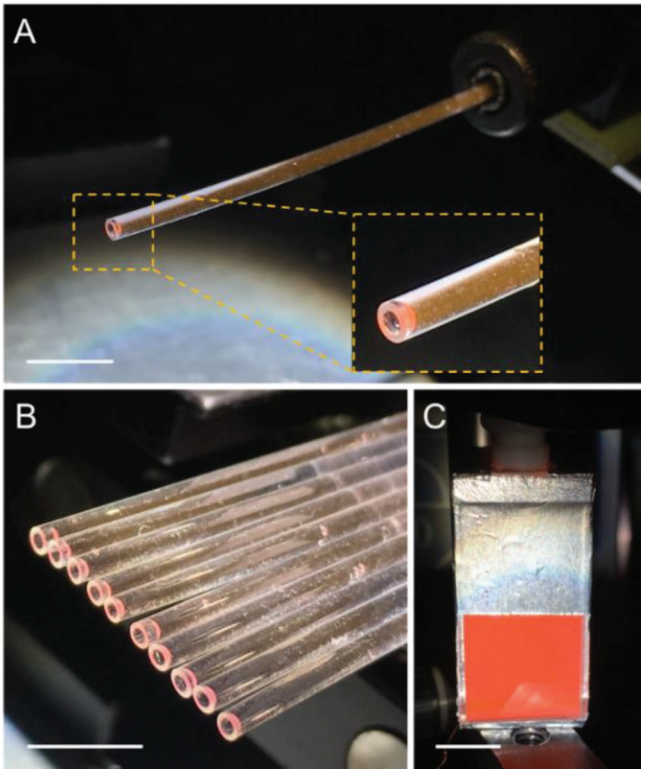

Figure 4. Photographs of A) a c-LSC based on the 17×10^{-7} M solution, B) a bundle structure of c-LSCs based on 4.2×10^{-7} M solution, and C) a p-LSC (with reflective tape) based on 3.3×10^{-7} M solution and under AM1.5G illumination (scale bars: 1×10^{-2} m).

where P_{out}^{el} and FF = 0.75 are the PV device output electrical power and fill factor, respectively. The effective contribution of this c-LSC on a PV device yielded a PCE value of $(3.2 \pm 0.1) \times 10^{-3}$%. We should note that losses of the guided light due to the bending of the fibers can be neglected, as negligible leakage losses are reported for POFs with a bending angle of 180° and a curvature radius higher than 30×10^{-3} m,[63] which was already considered valid for a POF-based LSC.[49]

The performance was also evaluated by measuring I_{SC}^{L} as function of the incident wavelength and calculating the EQE of the PV devices coupled to the c-LSCs. The EQE was calculated as follows

$$EQE(\lambda) = \frac{I_{SC} \cdot h \cdot c}{P_{in} \cdot e \cdot \lambda} \quad (5)$$

where e is the charge of the electron, h is the Planck's constant, c is the speed of light, and λ is the wavelength (Supporting Information for details). For all the c-LSCs tested, the maximum EQE values for the PV device are well correlated with the peaks found in the absorption spectra of the active layer (**Figure 7**; Figures S4–S6 in the Supporting Information), with the larger EQE variation between 500 and 600 nm. The maximum value of EQE = 0.1647 ± (0.0002)% was found for the c-LSC with $G \approx 7$ filled with the 4.2×10^{-7} M solution.

2.2. Bundle of c-LSCs and a p-LSC

The previous results point out that POFs filled with R-PE solutions can be used to fabricate c-LSCs and that the use of optically active centres dispersed in a liquid medium in LSCs presents some advantages when compared to the case of a solid matrix LSC. For instance, the concentration of the solutions can be easily varied,[8,36,38,43] liquids are easily moulded to the container geometry, the performance of the solar cells at the edges of the LSC is fixed and constant, removing the variability when comparing different fluorophores and concentrations,[43] and liquid solutions can be easily replaced when compared with materials that undergo a phase exchange to solid.[41]

To demonstrate the potential of these two approaches, it is necessary to enlarge A_s and, consequently, PCE values which will permit to envisage the application in PV cell to supply low-power consumption devices. Therefore, to enhance the PV cell performance in the presence of an LSC, A_s was increased following two methods: i) the assembling of c-LSCs into a bundle structure (Figure 4B; Figure S7 in the Supporting Information) and ii) p-LSC based on a glass container (Figure 4C).

The solutions with concentration values within 3.3×10^{-7} to 4.2×10^{-7} M combine larger emission quantum yield, brightness, and integral overlap, and, therefore, they were used to fabricate a bundle of c-LSCs and a p-LSC. When coupled to a Si-based PV device maximum η_{opt} values (Equation (2)) of 2.71 ± 0.07% and 5.6 ± 0.2% (4.74 ± 0.01% and 6.88 ± 0.01% when using Equation (3)), respectively, were found. These values are larger than those reported for c-LSCs formed by a single POF. Also, the PCE values found for the p-LSC and c-LSCs bundle were 0.27 ± 0.01% and $(23.03 \pm 0.02) \times 10^{-3}$%,

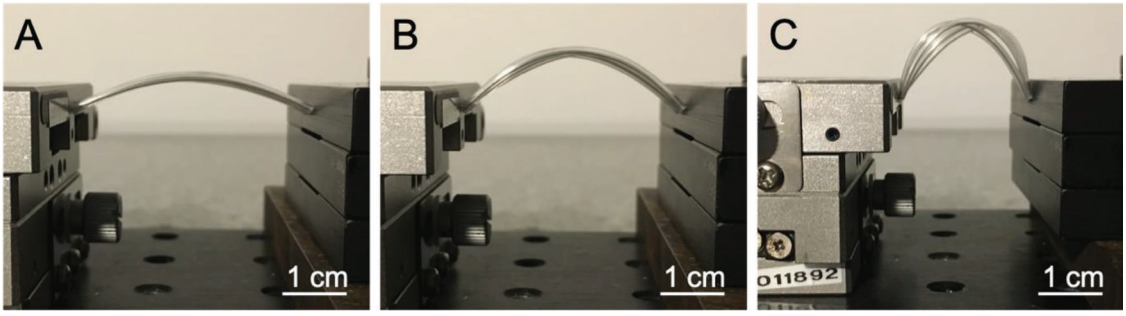

Figure 5. Photos of the bundle being bended showing the flexibility of the POFs.

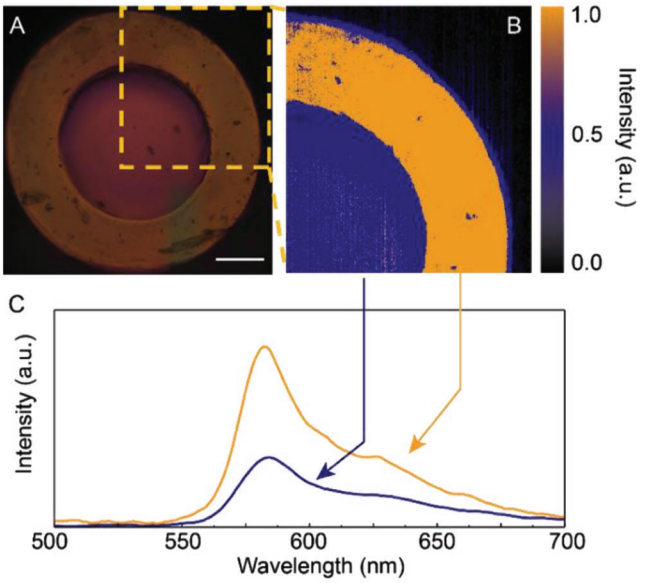

Figure 6. A) Cross-section optical microscopy images of a c-LSC under UV irradiation at 365 nm (scale bar: 3×10^{-4} m), B) hyperspectral image of a selected area, and C) corresponding emission spectra measured in the core and PMMA regions.

respectively. EQE measurements were performed showing good correlation with the absorption spectra, yielding maximum values of 2.7134 ± (0.0002)%, for the p-LSC (Figures S8 and S9 in the Supporting Information). It is worth noting that, considering LSCs based on natural organic dyes, the η_{opt} value of the p-LSC here reported is higher than the recently reported p-LSC based on chlorophyll with η_{opt} = 3.70%.[17] The η_{opt} and PCE values of the two types of LSCs fabricated in this work cannot be directly compared, as the absorption dependence of A_s was not considered (a calculus lying beyond the scope of this work).

As far as we know, only p-LSCs in which the optically active centres are dispersed in liquid medium were reported. Moreover, all the studies refer to the use of synthetic dyes or QDs in organic solvents, rather than natural dyes in water. Nevertheless, the η_{opt} values calculated in the present work are among the highest values in literature (**Table 2**). Higher values were only reported for LSC based on synthetic dyes (Rhodamine B,[41] Red F,[41,45] K_I, Sulphorhodamine 101, BASF-402, and BASF-241 dyes)[40] and PbS QDs.[42] Concerning PCE, care should be taken for comparison purposes, as it is dependent on the optical properties of the semiconductor used to fabricate the PV cell. For LSCs characterized with similar c-Si PV cells, the values here reported are lower than those reported for other LSCs with optically active centres dispersed in liquid medium (Table 2).

3. Modelling

Simulations of the performance (η_{opt}) of the p-LSC were carried out using a Monte Carlo ray-tracing approach, in which the photon propagation follows geometrical optical laws.[64–66] The

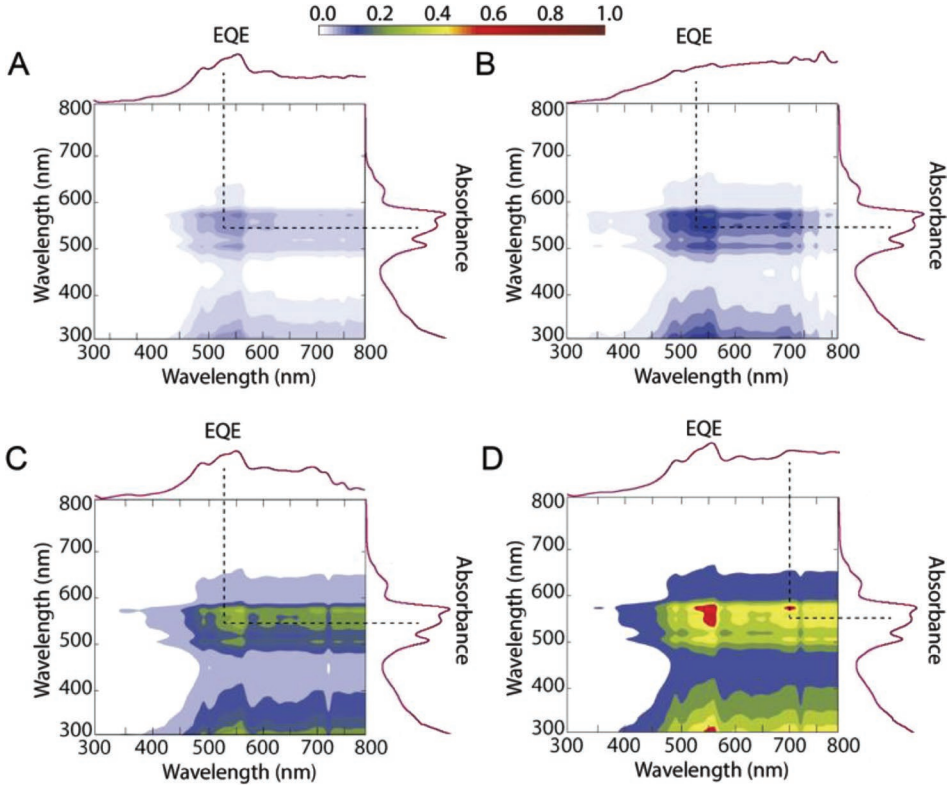

Figure 7. Cross correlation between the EQE of the photodiode coupled to the c-LSCs ($G \approx 9$) and the absorption spectrum of the correspondent R-PE solution for the illustrative examples of A) 4.2×10^{-7} M, B) 5.8×10^{-7} M, C) 7.5×10^{-7} M, and D) 17×10^{-7} M solutions. We note that increasing concentration the correlation is more evident. The colour-scale intensity is a measure of the correlation.

Table 2. η_{opt} (%) and PCE (%) values of the LSCs prepared here, the former values were calculated through Equation (2). For p-LSCs literature values of active centres dispersed in distinct liquid media are also listed for comparison. The concentration ([ ], M) of the active centres on the liquid media and the LSC surface area As ($l \times w$, cm^2) are also presented.

	Medium	Active centre	[ ]	A_s	η_{opt}	PCE	Ref.
c-LSCs bundle	Water	R-PE	4.2×10^{-7}	3.5×1.4	4.74	0.02 (Si)	This work
p-LSC	Water	R-PE	3.3×10^{-7}	2.0×2.0	6.88	0.27 (Si)	
	PPC/EG	Rhodamine B	–	2.5×7.6	15.3	–	[1]
		LDS698			3.6		
		LDS821	$\approx 10^{-4}$		2.9		
	Cl-benzene	MDMO-PPV	$\approx 10^{-3}$		5.9		
		MEH-DOO-PPV	–		5.0		
		Red F	8×10^{-6}		19.8		
	Toluene	CdSe/ZnS	3×10^{-6}		1.6		
	TX-100	K_l	–	5×10	20.2	–	[2]
		Sulphorhodamine 101			18.2		
		BASF-402			19.7		
		BASF-241			13.9		
	Toluene	CdSe/ZnS	3×10^{-6}	4.5×1.2	0.5	1.2 (Si)	[3]
		PbS	1.93×10^{-4}		12.6	3.2 (Si)	
	LC E7	Coumarine/perylene	8×10^{-3}	5×5	3.2[a)]	–	[4]
	Toluene	Lumogen F Red 300	4×10^{-3}	2×2	12.0	–	[5]
	Toluene	Lumogen Red 305	1.23×10^{-7}	10×3.5	–	2.3 (Si)	[6]

Liquid crystal Nematic = LC E7, TX-100 = polymer Triton X-100, PPC = propylene carbonate, EG = ethylene glycol, Cl-bez = chlorobenzene; [a)]η_{opt} is simply defined as $\eta_{opt} = P_{out}/P_{in}$, without mentioning the definition behind it.

thickness of the active layer ($\approx 10^{-2}$ m) is much larger than that of the light coherent length ($\approx 10^{-7}$ m), thus, interference effects were neglected. The stochastic nature of the model is assured by the use of a variable seed in the random function used to describe the photons interactions and is also reflected in the fact that the propagated rays cannot split when reaching an interface but rather either transmitted or reflected, as predicted by Fresnel laws. We also note that light polarization is not taken into account. By modelling the path of each propagated ray, it is possible to know whether the photons are trapped inside the LSC, absorbed by the luminescent species, lost due to the escape cone and if they were collected at the edges of the LSC.

The input of the Monte Carlo ray-tracing simulation consists in photons following the solar spectrum probability density function AM1.5G (280–1600 nm, photons with angle of incidence between –45° and 45°), the absorption and emission spectra, the absolute emission quantum yield and refractive index of the R-PE aqueous solutions ($n \approx 1.3335$), and the dispersion curve of the cuvette glass (Figure S10 in the Supporting Information). Furthermore, we consider a thin layer of air underneath the LSC.

This model does not include individual molecules or optically active centres but applies statistical averaging of the absorption. First, the absorption probability is calculated by $p_{abs} = 1–10^{-\alpha d}$, where α is the attenuation coefficient (in cm^{-1}) and d is the photon desired step size (0.02 cm) in each iteration, as function of the wavelength and compared with a random generated number between 0 and 1 for each launched photon. If p_{abs} proves to be higher than the random number, the photon is absorbed, otherwise the photon continues to propagate according to its direction vector. Once a photon is absorbed, the subsequent fate of the excitation (that is, emission or nonradiative relaxation) is again determined by the Monte Carlo sampling according to the emission quantum yield. The direction of the emission is randomly distributed and the emission wavelength is sampled randomly from the normalized emission spectrum. The fate of each photon is either loss due to nonradiative recombination or escape from the LSC from the incident light interface. When a photon hits the PV interface, it counts as a PV absorption and the wavelength of the photon and its position on the PV interface is recorded.

The η_{opt} for simulation purposes is defined by the energy emitted (per unit of time) from the edge of the LSC divided by the solar energy falling on the p-LSC (per unit of time), as stated in Equation (2). The simulations (10^6 photons) were performed for a p-LSC with dimensions of $2.00 \times 2.00 \times 1.00$ cm^3 and as function of the concentration of the R-PE solution. The optical conversion efficiency was predicted for solutions of R-PE with all the concentrations tested considering all the photons reaching the edge and considering only the converted photons (Table S2 in the Supporting Information).

Takin into consideration the integral overlap (O, Table 1) and simulation results (Table S2 in the Supporting Information), the 3.3×10^{-7} M solution displays the better optical performance at lower dye concentration and that was the rationale behind

the selection of this solution for the fabrication of the p-LSC. In this case, we highlight that the simulated η_{opt} values for the 3.3×10^{-7} M solution (6.28%) are slightly larger than those experimentally determined (5.6 ± 0.2%), pointing out that the device may be further optimized, particularly the PV cell coupling.[64,67]

4. Conclusions

In this work, natural-based LSCs made of R-PE aqueous solutions were studied. These optically active centres display large overlap with the solar irradiance on Earth (absorption at 300–700 nm) and emission spectra centred around 580 nm. Moreover, these aqueous solutions present the highest molar brightness values reported so far for organic dye molecules emitting in the 530–650 nm range, and thus LSCs based on R-PE aqueous solutions with distinct concentrations (4.2×10^{-8}–1.7×10^{-6} M) were tested. The best performance (η_{opt} and PCE values) was found for c-LSCs ($G \approx 7$) filled with the aqueous solutions with R-PE concentration of 4.2×10^{-7} M. Also, the POF-based c-LSCs were assembled in a bundle structure, yielding η_{opt} and PCE values of ≈4.74% and ≈23.03×10^{-3}%, respectively. Nevertheless, the top performance device reported in this work was a p-LSC based on a glass cuvette, with η_{opt} and PCE values of ≈6.88% and ≈0.27%, respectively. These values are a starting point for the use of natural dyes as optical active centres for sustainable LSCs, demonstrating the potential of nature-inspired LSCs as a relevant step toward cheap and sustainable PV energy conversion.

5. Experimental Section

Materials: The red macroalgae *Gracilaria sp*. was grown in a land-based integrated aquaculture system at ALGAplus—Produção e Comercialização de Algas e seus Derivados, a company specialized in the production of macroalgae, located in Ílhavo, Portugal. The ammonium sulphate (99.5%) used in phycobiliproteins precipitation was purchased at Merck. A commercial standard of R-phycoerythrin (≥10.0 mg mL^{-1}) was purchased at Sigma-Aldrich.

Solid–Liquid Extraction: The solid–liquid extraction procedure used in this work was adapted from the methodology already proposed by Martins et al.[46] Briefly, after the harvesting of the macroalgae, the samples were cleaned and washed with fresh and distilled water at least 3 times to eliminate small particles and residues from the cultivation. The biomass was then stored at –20 °C. When needed, the macroalgae samples were frozen in liquid nitrogen and grounded to increase the contact surface, thus enhancing the extraction. The biomass was homogenized in distilled water at a solid–liquid ratio of 0.5 (weight of biomass per volume of solvent). Then, the solid–liquid extraction was performed with water at 250 rpm in an incubator (IKA KS 4000 ic control) protected from light exposure, during 20 min at room temperature. At the end of this step, a pinkish solution was obtained, filtered, and centrifuged in a Thermo Scientific Heraeus Megafuge 16 R centrifuge at 5000 rpm for 30 min at 4 °C. The resultant pellet was discarded while the phycobiliprotein-based pinkish supernatant was collected. An ammonium sulphate aqueous solution at 30% was used to pretreat the crude extract rich in phycobiliproteins obtained from the solid–liquid extraction performed. This step was realized aiming at the elimination of some of the contaminant proteins extracted simultaneously with the phycobiliproteins. With this stage, it was also possible to identify the potential effect of the purity level of the phycobiliproteins-rich extract as optically active centres in LSCs. After the pretreatment, the salt was dissolved and the solution was left at 4 °C for 4 h, being then centrifuged at 5000 rpm for 30 min at 4 °C. After the precipitation of the target proteins, the pellet was resuspended in distilled water at different concentrations. The phycobiliproteins concentration of each extract was calculated using a UV–Vis microplate reader (Synergy HT microplate reader—BioTek) at 565 nm and a calibration curve previously established for the commercial standard R-PE.

LSCs Fabrication: The c-LSCs were based on hollow-core POFs with distinct diameter values (Figure 1A), resulting in different geometrical gain factors (G), which is given by the ratio between the exposed (A_s) and edge (A_e) areas. The POFs were fabricated using a semi-industrial optical fiber manufacturing facility[49] and cut into segments with length $l \approx 5 \times 10^{-2}$ m. The hollow-core was filled with the R-PE solutions with a syringe. The edge coupled to the PV device was sealed with the polymeric resin NOA68, while the opposite one was kept open. The individual POFs were, then, assembled into bundles (Figure 1A). The p-LSCs were fabricated using an optical glass cuvette (CM Scientific) with dimensions tailored to fit the PV cell surface, as illustrated in Figure 1B. A total number of 39 and 4 c-LSCs and p-LSCs, respectively, were fabricated.

UV/Visible Absorption: UV/visible absorption spectra of the R-PE solutions were measured using a Lambda 950 dual-beam spectrometer (Perkin-Elmer). All measurements were performed using a 1 cm square quartz cell. Using the Beer–Lambert law, the molar extinction coefficient (ε, M^{-1} cm^{-1}) was calculated from the linear dependence (slope) found for absorbance versus concentration.

Photoluminescence Spectroscopy: The photoluminescence spectra were recorded at room temperature with a modular double-grating excitation spectrofluorimeter with a TRIAX 320 emission monochromator (Fluorolog-3, Horiba Scientific) coupled to a R928 Hamamatsu photomultiplier.

Absolute Emission Quantum Yield: The absolute emission quantum yield values (q) were measured at room temperature using a C9920-02 Hamamatsu system.[68] The method is accurate within 10%. The reference measurement was performed with an empty 1 cm square quartz cell, as the interest was the emission quantum yield value of the aqueous solution, rather than of the R-PE emitting centres alone.

Refractive Index: The refractive index values of the R-PE solutions were measured using an Abbemat 200, Anton Paar refractometer. Refractive index results are relative to 589 nm, a temperature of 22 °C and accurate to ±10^{-4}.

Optical Conversion Efficiency (η_{opt}) and PCE: The η_{opt} and PCE values here reported were measured at least three times (including for R-PE solutions prepared at different times) and the results were reproducible with a standard deviation of ±4%. All η_{opt} and PCE values reported in this manuscript present an absolute error inferred through Equations (S8) and (S9) in the Supporting Information. All performance measurements were done under standard simulated AM1.5G radiation (solar simulator model 10500, Abet Technologies).

EQE: The solar simulator was coupled to a monochromator (Triax 180, Horiba Scientific). The I_{sc} and P_{in} values were measured using a sourcemeter (2400 SourceMeter SMU Instruments, Keithley) and a c-Si calibrated photodiode (FDS1010, Thorlabs), respectively. The reported EQE values present an absolute error inferred through Equation (S12) in the Supporting Information.

Supporting Information

Supporting Information is available from the Wiley Online Library or from the author.

Acknowledgements

Portuguese funding was provided by Fundação para a Ciência e a Tecnologia (FCT), EU/FEDER COMPETE and Mais Centro-PORC,

under contracts PEST-OE/EEI/LA0008/2013 and CENTRO-07-ST24-FEDER-002032. This work was developed within the scope of the projects CICECO-Aveiro Institute of Materials, POCI-01-0145-FEDER-007679 (FCT Ref. UID/CTM/50011/2013), SusPhotoSolutions—Soluções Fotovoltaicas Sustentáveis, CENTRO-01-0145-FEDER-000005, Solar-Flex, CENTRO-01-0145-FEDER-030186, and Instituto de Telecomunicações (FCT Ref. UID/EEA/50008/2013), financed by funds through the FCT/MEC and when appropriate cofinanced by FEDER under the PT2020 Partnership Agreement. Solar-Flex is a bilateral FCT/Fundação de Amparo à Pesquisa do Estado de São Paulo, Brazil, project (2018/07727-7). The authors acknowledge ALGAPlus—Produção e Comercialização de Algas e seus Derivados for seaweed samples and A.R.F. and M.M. thank FCT for the PhD grants (PD/BD/114454/2016 and SFRH/BD/122220/2016, respectively). S.F.H.C. and S.P.M.V. thank SusPhotoSolutions for the postdoctoral grant and FCT for the IF (IF/00402/2015) contract, respectively.

Conflict of Interest

The authors declare no conflict of interest.

Keywords

bundles, luminescent solar concentrators, natural optically active center, organic–inorganic hybrids, R-phycoerythrin, sustainability

Received: October 12, 2018
Revised: December 13, 2018
Published online:

[1] X. Huang, S. Han, W. Huang, X. Liu, *Chem. Soc. Rev.* **2013**, *42*, 173.
[2] W. H. Weber, J. Lambe, *Appl. Opt.* **1976**, *15*, 2299.
[3] A. Goetzberger, W. Greubel, *Appl. Phys.* **1977**, *14*, 123.
[4] B. A. Swartz, T. Cole, A. H. Zewail, *Opt. Lett.* **1977**, *1*, 73.
[5] J. S. Batchelder, A. H. Zewail, T. Cole, *Appl. Opt.* **1979**, *18*, 3090.
[6] R. Reisfeld, S. Neuman, *Nature* **1978**, *274*, 144.
[7] A. Goetzberger, V. Wittwer, *Sol. Cells* **1981**, *4*, 3.
[8] G. Lifante, F. Cusso, F. Meseguer, F. Jaque, *Appl. Opt.* **1983**, *22*, 3966.
[9] D. R. Needell, O. Ilic, C. R. Bukowsky, Z. Nett, L. Xu, J. W. He, H. Bauser, B. G. Lee, J. F. Geisz, R. G. Nuzzo, A. P. Alivisatos, H. A. Atwater, *IEEE J. Photovoltaics* **2018**, *8*, 1560.
[10] M. Kanellis, M. M. de Jong, L. Slooff, M. G. Debije, *Renewable Energy* **2017**, *103*, 647.
[11] M. G. Debije, C. Tzikas, V. A. Rajkumar, M. M. de Jong, *Renewable Energy* **2017**, *113*, 1288.
[12] M. G. Debije, C. Tzikas, M. M. de Jong, M. Kanellis, L. H. Slooff, *Renewable Energy* **2018**, *116*, 335.
[13] B. McKenna, R. C. Evans, *Adv. Mater.* **2017**, *29*, 1606491.
[14] B. P. V. Heiz, Z. Pan, G. Lautenschlager, C. Sirtl, M. Kraus, L. Wondraczek, *Adv. Sci.* **2017**, *4*, 1600362.
[15] M. R. Bergren, N. S. Makarov, K. Ramasamy, A. Jackson, R. Gughelmetti, H. McDaniel, *ACS Energy Lett.* **2018**, *3*, 520.
[16] I. G. Lim, S. W. Kang, C. Hyoung, K. H. Park, S. E. Kim, T. W. Kang, H. I. Park, J. H. Hwang, B. G. Choi, T. Y. Kang, *US Patent: US20140015470A1*, **2014**.
[17] A. R. Frias, E. Pecoraro, S. F. H. Correia, L. M. G. Minas, A. R. Bastos, S. García-Revilla, R. Balda, S. J. L. Ribeiro, P. S. André, L. D. Carlos, R. A. S. Ferreira, *J. Mater. Chem. A* **2018**, *6*, 8712.
[18] E.-H. Banaei, A. F. Abouraddy, *Prog. Photovolt: Res. Appl.* **2015**, *23*, 403.
[19] K. R. McIntosh, N. Yamada, B. S. Richards, *Appl. Phys. B* **2007**, *88*, 285.
[20] S. F. H. Correia, A. R. Frias, L. Fu, R. Rondão, E. Pecoraro, S. J. L. Ribeiro, P. S. André, R. A. S. Ferreir, L. D. Carlos, *Adv. Sustainable Syst.* **2018**,*2*, 1800002.
[21] S. F. H. Correia, V. de Zea Bermudez, S. J. L. Ribeiro, P. S. André, R. A. S. Ferreira, L. D. Carlos, *J. Mater. Chem. A* **2014**, *2*, 5580.
[22] F. Purcell-Milton, Y. K. Gun'ko, *J. Mater. Chem.* **2012**, *22*, 16687.
[23] F. Meinardi, F. Bruni, S. Brovelli, *Nat. Rev. Mater.* **2017**, *2*, 17072.
[24] Y. M. Zhao, R. R. Lunt, *Adv. Energy Mater.* **2013**, *3*, 1143.
[25] R. Reisfeld, D. Shamrakov, C. Jorgensen, *Sol. Energy Mater. Sol. Cells* **1994**, *33*, 417.
[26] M. G. Debije, P. P. C. Verbunt, *Adv. Energy Mater.* **2012**, *2*, 12.
[27] A. Dey, S. A. Moyez, M. K. Mandal, S. Roy, *Mater. Today: Proc.* **2016**, *3*, 3498.
[28] N. J. L. K. Davis, R. W. MacQueen, S. T. E. Jones, C. Orofino-Pena, D. Cortizo-Lacalle, R. G. D. Taylor, D. Credgington, P. J. Skabara, N. C. Greenham, *J. Mater. Chem. C* **2017**, *5*, 1952.
[29] T. C. Han, J. J. Zhao, T. Yuan, D. Y. Lei, B. W. Li, C. W. Qiu, *Energy Environ. Sci.* **2013**, *6*, 3537.
[30] V. Fattori, M. Melucci, L. Ferrante, M. Zambianchi, I. Manet, W. Oberhauser, G. Giambastiani, M. Frediani, G. Giachi, N. Camaioni, *Energy Environ. Sci.* **2011**, *4*, 2849.
[31] C. L. Mulder, L. Theogarajan, M. Currie, J. K. Mapel, M. A. Baldo, M. Vaughn, P. Willard, B. D. Bruce, M. W. Moss, C. E. McLain, J. P. Morseman, *Adv. Mater.* **2009**, *21*, 3181.
[32] R. Bose, M. Gonzalez, P. Jenkins, R. Walters, J. Morseman, M. Moss, C. McLain, P. Linsert, A. Buchtemann, A. J. Chatten, K. W. J. Barnham, *35th IEEE Photovoltaic Specialists Conference* **2010**, 467.
[33] A. N. Glazer, *Methods Enzymol.* **1988**, *167*, 291.
[34] R. Bose, M. Gonzalez, P. Jenkins, R. Walters, J. Morseman, M. Moss, C. McLain, P. Linsert, A. Buchtemann, A. J. Chatten, K. W. J. Barnham, presented at *IEEE Phot. Spec. Conf.*, Honolulu, USA, June **2010**.
[35] L. R. Bradshaw, K. E. Knowles, S. McDowall, D. R. Gamelin, *Nano Lett.* **2015**, *15*, 1315.
[36] M. S. Decardona, M. Carrascosa, F. Meseguer, F. Cusso, F. Jaque, *Appl. Opt.* **1985**, *24*, 2028.
[37] K. E. Knowles, T. B. Kilburn, D. G. Alzate, S. McDowall, D. R. Gamelin, *Chem. Commun.* **2015**, *51*, 9129.
[38] R. Kondepudi, S. Srinivasan, *Sol. Energy Mater.* **1990**, *20*, 257.
[39] Z. Krumer, S. J. Pera, R. J. A. van Dijk-Moes, Y. M. Zhao, A. F. P. de Brouwer, E. Groeneveld, W. G. J. H. M. van Sark, R. E. I. Schropp, C. D. Donega, *Sol. Energy Mater. Sol. Cells* **2013**, *111*, 57.
[40] A. F. Mansour, *Polym. Test.* **1998**, *17*, 153.
[41] V. Sholin, J. D. Olson, S. A. Carter, *J. Appl. Phys.* **2007**, *101*, 123114.
[42] G. V. Shcherbatyuk, R. H. Inman, C. Wang, R. Winston, S. Ghosh, *Appl. Phys. Lett.* **2010**, *96*, 191901.
[43] M. Gajic, F. Lisi, N. Kirkwood, T. A. Smith, P. Mulvaney, G. Rosengarten, *Sol. Energy* **2017**, *150*, 30.
[44] J. A. H. P. Sol, V. Dehm, R. Hecht, F. Würthner, A. P. H. J. Schenning, M. G. Debije, *Angew. Chem., Int. Ed.* **2017**, *56*, 1.
[45] A. L. Rodarte, F. Cisneros, L. S. Hirst, S. Ghosh, *Liq. Cryst.* **2014**, *41*, 1442.
[46] M. Martins, F. A. Vieira, I. Correia, R. A. S. Ferreira, H. Abreu, J. A. P. Coutinho, S. P. M. Ventura, *Green Chem.* **2016**, *18*, 4287.
[47] J. F. Niu, M. L. Xu, G. C. Wang, K. Y. Zhang, G. Peng, *Indian J. Geo-Mar. Sci.* **2013**, *42*, 21.
[48] J. A. Rivera, J. G. Eden, *APL Photonics* **2017**, *2*, 121301.
[49] S. F. H. Correia, P. P. Lima, E. Pecoraro, S. J. L. Ribeiro, P. S. André, R. A. S. Ferreira, L. D. Carlos, *Prog. Photovoltaics* **2016**, *24*, 1178.
[50] M. J. Currie, J. K. Mapel, T. D. Heidel, S. Goffri, M. A. Baldo, *Science* **2008**, *321*, 226.
[51] R. Reisfeld, *Opt. Mater.* **2010**, *32*, 850.

[52] S. P. M. Ventura, F. A. E. Silva, M. V. Quental, D. Mondal, M. G. Freire, J. A. P. Coutinho, *Chem. Rev.* **2017**, *117*, 6984.
[53] K. S. Rowan, *Photosynthetic Pigments of Algae*, CUP Archive, Cambridge University Press **1989**.
[54] V. V. Egorov, *Int. Conf. Lumin. Opt. Spectrosc. Condens. Matter* **2009**, *2*, 223.
[55] R. MacColl, L. E. Eisele, E. C. Williams, S. S. Bowser, *J. Biol. Chem.* **1996**, *271*, 17157.
[56] V. T. Oi, A. N. Glazer, L. Stryer, *J. Cell Biol.* **1982**, *93*, 981.
[57] D. J. W. Barber, J. T. Richards, *Photochem. Photobiol.* **1977**, *25*, 565.
[58] R. Rondão, A. R. Frias, S. F. H. Correia, L. Fu, V. de Zea Bermudez, P. S. André, R. A. S. Ferreira, L. D. Carlos, *ACS Appl. Mater. Interfaces* **2017**, *9*, 12540.
[59] P. Reineck, A. Francis, A. Orth, D. W. M. Lau, R. D. V. Nixon-Luke, I. Das Rastogi, W. A. W. Razali, N. M. Cordina, L. M. Parker, V. K. A. Sreenivasan, L. J. Brown, B. C. Gibson, *Adv. Opt. Mater.* **2016**, *4*, 1549.
[60] R. Hein, R. Y. Tsien, *Curr. Biol.* **1996**, *6*, 178.
[61] A. N. Butkevich, V. N. Belov, K. Kolmakov, V. V. Sokolov, H. Shojaei, S. C. Sidenstein, D. Kamin, J. Matthias, R. Vlijm, J. Engelhardt, S. W. Hell, *Chem. - Eur. J.* **2017**, *23*, 12114.
[62] H. M. Zidan, M. Abu-Elnader, *Phys. B* **2005**, *355*, 308.
[63] J. H. Kuang, P. C. Chen, Y. C. Chen, *Sensors* **2010**, *10*, 10198.
[64] F. Meinardi, S. Ehrenberg, L. Dhamo, F. Carulli, M. Mauri, F. Bruni, R. Simonutti, U. Kortshagen, S. Brovelli, *Nat. Photonics* **2017**, *11*, 177.
[65] H. Hernandez-Noyola, D. H. Potterveld, R. J. Holt, S. B. Darling, *Energy Environ. Sci.* **2012**, *5*, 5798.
[66] M. Portnoi, C. Sol, C. Tummeltshammer, I. Papakonstantinou, *Opt. Lett.* **2017**, *42*, 2695.
[67] L. H. Slooff, E. E. Bende, A. R. Burgers, T. Budel, M. Pravettoni, R. P. Kenny, E. D. Dunlop, A. Büchtemann, *Phys. Status Solidi RRL* **2008**, *2*, 257.
[68] V. T. Freitas, P. P. Lima, R. A. S. Ferreira, E. Pecoraro, M. Fernandes, V. de Zea Bermudez, L. D. Carlos, *J. Sol-Gel Sci. Technol.* **2013**, *65*, 83.